

Referring Expression Instance Retrieval and A Strong End-to-End Baseline

Xiangzhao Hao*

haoxiangzhao2023@ia.ac.cn
Institute of Automation, Chinese
Academy of Sciences
Beijing, China

Kuan Zhu*

kuan.zhu@nlpr.ia.ac.cn
Institute of Automation, Chinese
Academy of Sciences
Beijing, China

Hongyu Guo

23120800@bjtu.edu.cn
Institute of Automation, Chinese
Academy of Sciences
Beijing, China

Haiyun Guo

haiyun.guo@nlpr.ia.ac.cn
Institute of Automation, Chinese
Academy of Sciences
Beijing, China

Ning Jiang

ning.jiang02@msxf.com
Mashang Consumer Finance Co, Ltd
Chongqing, China

Quan Lu

quan.lu02@msxf.com
Mashang Consumer Finance Co, Ltd
Chongqing, China

Ming Tang

tangm@nlpr.ia.ac.cn
Institute of Automation, Chinese
Academy of Sciences
Beijing, China

Jinqiao Wang[†]

jqwang@nlpr.ia.ac.cn
Institute of Automation, Chinese
Academy of Sciences
Beijing, China

Abstract

Using natural language to query visual information is a fundamental need in real-world applications, which has inspired a wide range of vision-language tasks. Text-Image Retrieval (TIR) retrieves a target image from a gallery based on an image-level description, while Referring Expression Comprehension (REC) localizes a target object within a given image using an instance-level description. However, real-world applications often present more complex demands. Users typically query an instance-level description across a large gallery and expect to receive both relevant image and the corresponding instance location. In such scenarios, TIR struggles with fine-grained descriptions and object-level localization, while REC is limited in its ability to efficiently search large galleries and lacks an effective ranking mechanism. In this paper, we introduce a new task called **Referring Expression Instance Retrieval (REIR)**, which supports both instance-level retrieval and localization based on fine-grained referring expressions. First, we propose a large-scale benchmark for REIR, named **REIRCOCO**, constructed by prompting advanced vision-language models to generate high-quality referring expressions for instances in the MSCOCO and RefCOCO datasets. Second, we present a baseline method, **Contrastive Language-Instance Alignment with Relation Experts (CLARE)**, which employs a dual-stream architecture to address REIR in an end-to-end manner. Given a referring expression, the textual branch encodes it into a query embedding, enhanced by a Mix of Relation Experts (MORE) module designed to better capture inter-instance relationships. The visual branch detects candidate objects and extracts their instance-level visual features. The most similar candidate to the query is selected for bounding box prediction. CLARE is first trained on object detection and REC datasets to establish initial grounding capabilities, then

optimized via Contrastive Language-Instance Alignment (CLIA) for improved retrieval across images. Experimental results demonstrate that CLARE outperforms existing methods on the REIR benchmark and generalizes well to both TIR and REC tasks, showcasing its effectiveness and versatility. We will release our code and benchmark publicly.

1 Introduction

Querying visual information using natural language is a fundamental and widely demanded capability in vision-language systems. Existing efforts in this area are often categorized into two representative tasks based on the granularity of the textual query and the scope of visual search. **Text-Image Retrieval (TIR)** aims to retrieve relevant images from a gallery using image-level captions. Recent TIR methods typically adopt large-scale contrastive learning between paired images and texts [27, 38, 41, 54], enabling strong global retrieval performance. **Referring Expression Comprehension (REC)**, in contrast, focuses on localizing a specific object instance within a single image based on fine-grained referring expressions. State-of-the-art REC models usually rely on early cross-modal fusion modules to align image and text features, followed by decoder heads to predict the location of the referred object [9, 46, 48, 50]. These differences in task scope and methodology are illustrated in Figure 1.

However, real-world applications such as surveillance retrieval, image forensics, and personal photo search often demand a hybrid capability: given an instance-level natural language expression, the system should directly retrieve and localize the corresponding object instance from a large image gallery. Such expressions typically describe salient objects using both appearance and relational context, e.g., *The brown dog lies on a cushion near the fireplace with a red rug underneath*. Unfortunately, while existing TIR methods are efficient, they lack localization capabilities and fail to identify

*Both authors contributed equally to this research.

[†]Corresponding author.

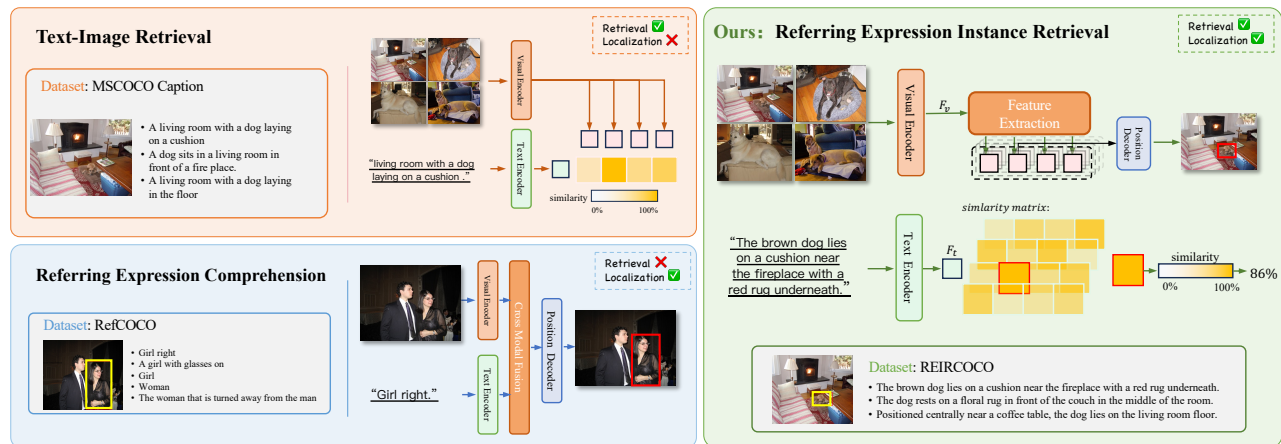


Figure 1: Comparison of three vision-language tasks and their datasets. REIR enables end-to-end instance-level retrieval and localization, addressing the limitations of Text-Image retrieval and Referring Expression Comprehension.

specific object instances. REC models, in contrast, offer precise localization within a single image but rely on expensive cross-modal feature fusion and are impractical for gallery-wide retrieval. Moreover, neither task provides a unified evaluation protocol for jointly assessing retrieval and grounding performance.

To address these limitations, we propose a new task: **Referring Expression Instance Retrieval (REIR)**. REIR requires models to *directly retrieve and localize the referred object instance from a gallery of images*, based on a fine-grained natural language expression. To support this task, we introduce a new dataset, **REIRCOCO**, which provides high-quality instance-level expressions paired with precise bounding box annotations. As illustrated in Figure 1, existing datasets are not suitable for this task. TIR datasets like MSCOCO Captions [6] only contain image-level descriptions (e.g., *A living room with a dog lying on a cushion*) without object-level annotations, while REC datasets such as RefCOCO [20, 53] rely on short, ambiguous expressions (e.g., *Girl*) that can refer to multiple targets in gallery settings. In contrast, REIRCOCO offers fine-grained and unambiguous expressions (e.g., *The brown dog lies on a cushion near the fireplace with a red rug underneath*), uniquely grounding specific object instances even in cluttered scenes. We construct REIRCOCO using an automated pipeline with two stages: generation and filtering. In the generation stage, we prompt a vision-language model to produce contextualized referring expressions for each object in the MSCOCO detection dataset [29] and RefCOCO dataset. Each prompt incorporates the object’s attributes, spatial relations, and surrounding context to encourage relationally rich and instance-specific descriptions. In the filtering stage, a separate language model evaluates expression quality, removing samples that are ambiguous, inaccurate, or non-discriminative. The resulting dataset contains over 30,000 images and 200,000 uniquely annotated object instances, each paired with several fine-grained referring expressions that unambiguously correspond to a single target.

To address the REIR task, we propose a new end-to-end model named **CLARE** (Contrastive Language-Instance Alignment with Relation Experts). CLARE adopts a dual-stream architecture that

decouples text and image encoding for efficient cross-modal alignment. Given a referring expression, the text encoder produces a sentence-level embedding, which is refined by a **Mix of Relation Experts (MORE)** module to enhance relational semantics. In parallel, the visual encoder extracts instance-level object features, which encapsulate not only the appearance attributes of each object but also their spatial and contextual relationships within the image. To align the two modalities, we introduce **Contrastive Language-Instance Alignment (CLIA)** module, a contrastive learning objective that matches textual queries with object candidates across images using the SigLIP loss [54]. This enables CLARE to effectively align instance-level visual features with referring expressions, allowing the model to identify the most relevant object among all candidate instances across the gallery, thereby achieving simultaneous retrieval and localization.

To evaluate our approach, we construct strong baselines by combining and adapting representative TIR and REC methods in the REIR setting, and these adapted methods perform poorly. We compare these baselines with our proposed CLARE under standardized settings and observe that CLARE achieves consistently superior performance on the REIR task. Extensive ablation studies further validate the effectiveness of both our proposed model and the REIRCOCO dataset. Furthermore, CLARE also performs competitively on traditional REC and TIR benchmarks, demonstrating strong generalization across vision-language tasks. Our main contributions are summarized as follows:

- We introduce a new task, **Referring Expression Instance Retrieval (REIR)**, which better reflects real-world vision-language demands and extends the scope of traditional retrieval and grounding tasks.
- We construct a large-scale dataset, **REIRCOCO**, where each object instance is annotated with a semantically rich instance-level referring expression. To the best of our knowledge, this is the first dataset specifically designed for instance-level retrieval and localization in open-world scenarios.
- We propose **CLARE** (Contrastive Language-Instance Alignment with Relation Experts), an end-to-end framework that

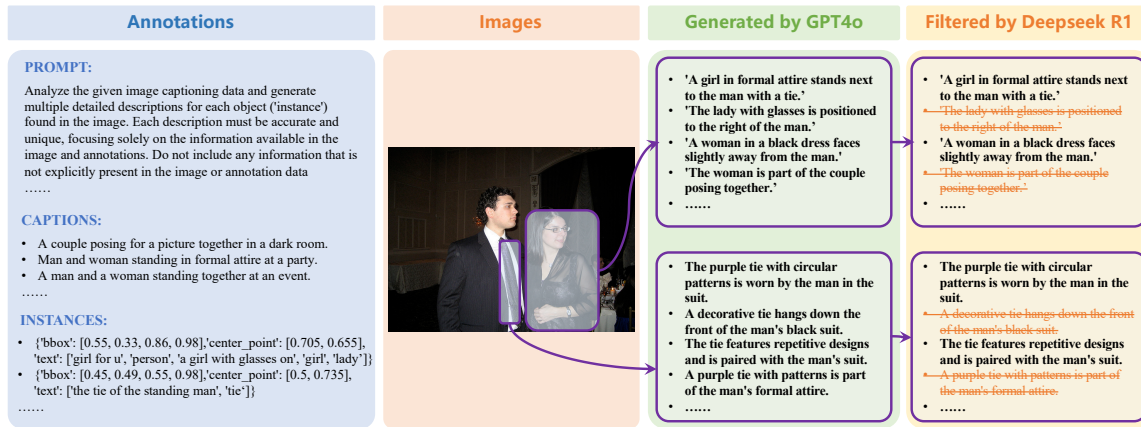


Figure 2: Overview of the REIRCOCO dataset construction pipeline. GPT-4o produces context-rich and uniquely grounded referring expressions for annotated instances using structured prompts. DeepSeek R1 verifies expression quality and removes ambiguous or low-informative samples.

enables simultaneous retrieval and localization through instance-level language-object contrastive alignment.

- We conduct extensive experiments on REIR, TIR, and REC benchmarks. CLARE achieves state-of-the-art performance on the REIR task, while also demonstrating strong generalization capabilities on traditional REC and TIR settings.

2 Related Works

2.1 Referring Expression Comprehension

Referring Expression Comprehension (REC) aims to localize a specific object within a given image based on a natural language expression. Existing approaches are typically classified into two-stage and one-stage paradigms, mainly distinguished by whether they perform early fusion of visual and textual features. **Two-stage methods** [15, 17, 32, 33, 49, 52] detect object proposals using pre-trained object detectors such as Faster R-CNN [39], and then compute cross-modal similarity between each region and the referring expression. These methods benefit from modularity and interpretability, but generally lack deep feature fusion and end-to-end optimization. As a result, they struggle to model complex relationships or semantic nuances, especially in open-world or gallery-level settings. **One-stage methods** [11, 19, 46, 50, 57] bypass the proposal stage by jointly encoding images and text through early fusion in a unified architecture. With the rise of vision-language transformers [42] and large-scale pretrained multimodal models (MLLMs) [2, 5, 47, 51], one-stage methods have demonstrated superior performance across multiple benchmarks, largely due to their stronger representation learning and global reasoning capacity.

However, most REC methods rely on early feature fusion, which requires recomputing cross-modal features for each text-image pair. This makes them inefficient for large-scale gallery retrieval. In contrast, our method adopts a contrastive language-instance alignment strategy that enables effective grounding *without requiring explicit feature fusion*. As a result, it achieves competitive or even superior grounding performance while maintaining scalability across large image galleries.

2.2 Text-Image Retrieval

Text-Image Retrieval (TIR) aims to retrieve the most relevant image from a gallery based on a natural language query. Early approaches [12, 13, 36] constructed joint embedding spaces using handcrafted or CNN-based features, but these methods lacked semantic understanding and showed poor generalization. To address these limitations, some later works [23, 31, 44, 45] introduced object detectors to extract region-level features, enabling word-region matching. For example, SCAN [23] aligns detected image objects with textual fragments to improve retrieval precision. The current dominant paradigm is Vision-Language Pretraining (VLP), which leverages large-scale image-text pairs and self-supervised objectives [3, 22, 26]. These models are typically divided into two categories: one-stream and two-stream architectures. One-stream models [7, 14, 21, 55] jointly encode image regions and text tokens through a unified transformer for dense cross-modal interaction. In contrast, two-stream models [18, 25, 27, 37, 43] such as CLIP [38], EVA-CLIP [41], and SigLIP [54], encode images and texts independently and align them through contrastive learning, enabling efficient large-scale retrieval.

Despite their effectiveness, most TIR models focus on image-level alignment and lack explicit modeling of object-level semantics. This limitation motivates us to extend contrastive alignment to the instance level, enabling retrieval and localization of fine-grained targets as required by REIR.

3 Referring Expression Instance Retrieval

3.1 Task Definition

Referring Expression Instance Retrieval (REIR) is a unified vision-language task that requires models to *directly retrieve and localize* a referred object instance from a large-scale image gallery, given a natural language query.

Formally, given a referring expression x_{text} and a gallery of N images $\{x_{\text{img}}^i\}_{i=1}^N$, the model is required to predict a bounding box $B = [x, y, w, h]$ for the referred object, which need to lie within the

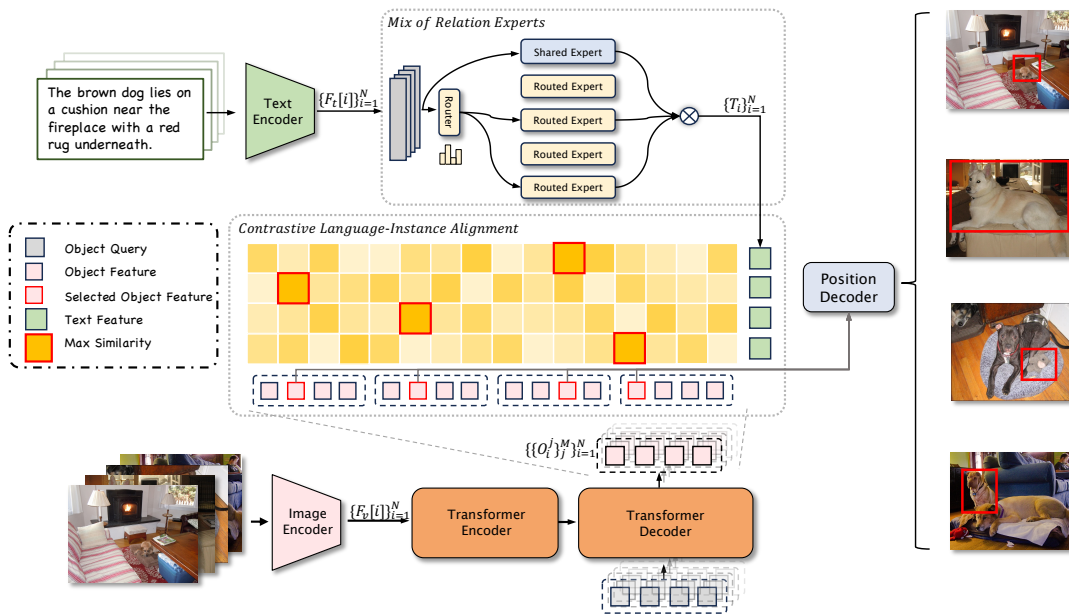


Figure 3: An overview of CLARE. The model encodes texts and images in parallel, then aligns referring expressions with instance-level object features via a Mix of Relation Experts (MORE) module and a Contrastive Language-Instance Alignment (CLIA) objective. This enables unified retrieval and localization across large-scale image galleries.

correct image x_{img}^i that contains the target instance. The model receives no prior information about which image contains the object, it needs to reason over all candidates to jointly determine both *where* and *what* to localize.

For instance, given the query “The brown dog lies on a cushion near the fireplace with a red rug underneath,” the model must retrieve the correct image from a large gallery and localize the exact dog being described. This is particularly challenging because many distractors may exist across the gallery—such as dogs lying on sofas, dogs outdoors, or images containing multiple dogs. The model must accurately match fine-grained appearance and contextual cues to locate the referred instance. As illustrated in Figure 1, this requires both precise retrieval and localization in the presence of semantically similar but incorrect candidates.

3.2 A New Dataset: REIRCOCO

To support the proposed REIR task, we construct a large-scale dataset named **REIRCOCO**, specifically designed for instance-level retrieval and localization. Unlike existing datasets, REIRCOCO features fine-grained and uniquely aligned textual descriptions for individual object instances, ensuring that each expression corresponds to exactly one target. This eliminates ambiguous references and negative truths, enabling accurate instance-level evaluation.

As illustrated in Figure 2, REIRCOCO is built through a scalable two-stage pipeline powered by vision-language foundation models: *generation* and *filtering*. In the **generation stage**, we begin with object annotations from the COCO detection and RefCOCO datasets. For each target instance, we construct structured prompts that include its bounding box, category label, the image’s global caption, and contextual information about surrounding objects.

These prompts are then passed to GPT-4o [1] to generate 5–10 diverse referring expressions per instance. To reduce the risk of *negative truths*—i.e., cases where a query unintentionally matches multiple similar objects across different images—the prompts are designed to maximize referential uniqueness. In particular, the model is encouraged to incorporate relational cues and spatial context involving nearby entities (e.g., “the chair to the left of the woman in red”) so that the generated expressions uniquely describe the target instance within the broader visual scene. This design ensures that each query expression has only one valid match in the entire image gallery, aligning perfectly with the REIR task requirement. In the **filtering stage**, we use DeepSeek R1 [10] to verify the quality of the generated descriptions. Each image is paired with a verification prompt that includes the caption and candidate expressions. The model is instructed to reject expressions that are ambiguous or semantically inconsistent with the image context, and to retain those that are specific, grounded, and discriminative. This automated filtering ensures that the final dataset contains only high-quality, retrieval-friendly expressions. See the Appendix for more details.

The resulting REIRCOCO dataset contains **30,106 images** and **215,835 object instances**, each annotated with multiple verified referring expressions—totaling **613,548 fine-grained descriptions**. Each expression is unambiguous and uniquely tied to a single instance, making the dataset well-suited for both retrieval and localization. Compared to prior datasets, REIRCOCO provides richer semantics, greater diversity, and stronger alignment with the REIR task objectives.

4 Contrastive Language-Instance Alignment with Relation Experts

4.1 Architecture Overview

As shown in Figure 3, our proposed model **CLARE** (*Contrastive Language-Instance Alignment with Relation Experts*) is an end-to-end dual-stream design tailored for instance-level retrieval and localization. It decouples vision and language processing while maintaining strong cross-modal alignment capabilities.

Given a batch of N image-text pairs $\{(x_{\text{text}}^i, x_{\text{img}}^i)\}_{i=1}^N$, the model processes each modality in parallel. On the visual side, each image x_{img}^i is passed through SigLIP vision encoder [54] to produce a dense feature map $F_v^i \in \mathbb{R}^{H \times W \times C}$. A Deformable-DETR-based object extractor is then applied to generate M object proposals and extract instance-level visual features $\{O_k^j\}_{j=1}^M \in \mathbb{R}^D$ by combining local appearance with global context using multi-scale deformable attention and Transformer decoding. These features encode both the visual appearance of each candidate object and its contextual relations within the scene, enabling the model to distinguish between visually similar instances in different spatial configurations. Simultaneously, the referring expression x_{text}^i is encoded into a sentence-level embedding F_t^i using the text encoder. This embedding is refined by the **MORE** module (*Mix of Relation Experts*) into $T_i \in \mathbb{R}^D$, which incorporates semantic, spatial, and inter-object relational cues. To perform instance-level alignment, we compute dot-product similarity scores between T_i and all object features O_k^l from the gallery. These scores are supervised by the proposed **CLIA** module (*Contrastive Language-Instance Alignment*), which extends SigLIP’s sigmoid-based contrastive objective to align referring expressions and object features across images. This allows the model to learn a unified similarity space for retrieval and localization. In addition, a Focal Loss is applied to supervise intra-image candidate selection and encourage discriminative matching.

4.2 Mix of Relation Experts

Referring expressions often combine both appearance cues and complex inter-object relationships. For example, “the man” captures a category-level visual concept, while “the man beside the woman in black” introduces spatial and relational context essential for disambiguating similar objects. To model this diversity, we propose the **Mix of Relation Experts (MORE)** module, which dynamically routes the global textual feature F_t^i through a mixture of experts.

Inspired by DeepSeek-MoE, the MORE module comprises two types of experts: *routed* and *shared experts*. The shared experts are always active and encode general semantics common across all expressions, while the routed experts are selectively activated based on each expression to specialize in fine-grained reasoning, such as spatial configurations, inter-object interactions, and comparative relations. Let N_s and N_r denote the number of shared and routed experts. The final text embedding is:

$$T_i = \sum_{j=1}^{N_s} \text{FFN}_j^{(s)}(F_t^i) + \sum_{k=1}^{N_r} \hat{g}_{k,i} \cdot \text{FFN}_k^{(r)}(F_t^i) \quad (1)$$

Routing weights $\hat{g}_{k,i}$ are obtained via a GatingNet:

$$g_i = \text{GatingNet}(F_t^i), \quad (2)$$

$$\hat{g}_{k,i} = \begin{cases} g_{k,i}, & \text{if } g_{k,i} \in \text{Top-}K_r(g_i) \\ 0, & \text{otherwise} \end{cases} \quad (3)$$

Only the top- K_r routed experts are activated per query to promote specialization and reduce redundancy. This design allows the model to dynamically adapt to diverse expression types and better encode the compositional semantics required for fine-grained retrieval and localization.

4.3 Contrastive Language-Instance Alignment

To support gallery-wide instance retrieval, we extend the sigmoid-based contrastive objective from SigLIP [54] to enable alignment between referring expressions and object-level visual features. This module, **Contrastive Language-Instance Alignment (CLIA)**, casts cross-modal matching as a binary classification task over all expression-object pairs across images and batches. Given a batch of B referring expressions T_i and all extracted object features O_k^l , we define the label $z_{i,k,l} = 1$ if the expression T_i refers to object O_k^l , and -1 otherwise. The CLIA loss is defined as:

$$\mathcal{L}_{\text{CLIA}} = -\frac{1}{B \cdot N} \sum_{i=1}^B \sum_{k=1}^B \sum_{l=1}^{N_k} \log \left(\frac{1}{1 + \exp(z_{i,k,l}(-t \langle T_i, O_k^l \rangle + b))} \right) \quad (4)$$

In which, $\langle \cdot, \cdot \rangle$ denotes dot-product similarity, t is a learnable temperature, and b is a bias scalar. By aligning each expression not only with objects in its paired image but also across other gallery images, CLIA encourages the model to learn globally discriminative instance-level features that reflect semantic, spatial, and relational consistency which enable robust retrieval and localization across large-scale datasets.

4.4 Training and Inference

Training. CLARE is trained in two phases. First, a pretraining phase builds basic recognition and alignment skills. Using COCO and RefCOCO, we apply Focal Loss and box regression to train the model without routed experts or CLIA.

$$\mathcal{L}_{\text{pretrain}} = \mathcal{L}_{\text{focal}} + \mathcal{L}_{\text{bbox}} \quad (5)$$

Then, a fine-tuning stage activates the full MORE module and applies CLIA loss on REIRCOCO:

$$\mathcal{L}_{\text{finetune}} = \mathcal{L}_{\text{CLIA}} + \mathcal{L}_{\text{focal}} + \mathcal{L}_{\text{bbox}} \quad (6)$$

Inference. CLARE supports scalable retrieval: instance-level features for all gallery images are precomputed. At test time, a query is encoded once and compared via dot product to all candidates, enabling efficient and accurate retrieval-localization without repeated fusion. This modular structure combines the flexibility of two-stream design with the fine-grained reasoning power of contrastive and expert-based modeling, making CLARE highly effective for the REIR task. See the Appendix for more details.

Table 1: Performance Comparison of Different Methods on the REIR Benchmark

Methods		$\tau = 0.5$			$\tau = 0.7$			$\tau = 0.9$		
		BR@1	BR@5	BR@10	BR@1	BR@5	BR@10	BR@1	BR@5	BR@10
TIR Methods	REC Methods	Two-Stage Method								
CLIP-ViT-B	deepseek-VL2-Tiny	11.15	21.84	26.89	8.98	18.00	23.50	5.32	10.51	13.48
CLIP-ViT-L	deepseek-VL2	13.31	26.45	32.79	12.85	25.41	31.53	11.02	21.42	26.50
CLIP-ViT-L	simVG-ViT-L	12.01	25.68	31.78	10.16	23.79	30.04	7.31	20.75	21.21
EVA-CLIP-ViT-B	deepseek-VL2-Tiny	12.82	24.58	29.52	11.56	21.08	25.18	6.05	12.42	14.80
EVA-CLIP-ViT-L	deepseek-VL2	16.38	29.89	36.21	15.77	28.73	34.78	13.32	24.18	29.15
EVA-CLIP-ViT-L	simVG-ViT-L	15.92	29.04	36.22	14.78	27.63	33.39	8.06	20.38	28.41
SIGLIP-ViT-B	deepseek-VL2-Tiny	15.26	27.43	32.93	13.27	23.60	28.34	7.63	13.53	16.09
SIGLIP-ViT-L	deepseek-VL2	18.52	33.22	39.48	17.82	31.90	37.84	15.04	26.74	31.50
SIGLIP-ViT-L	simVG-ViT-L	17.77	33.22	38.71	15.10	31.42	35.99	8.74	25.27	27.41
		End to End Method								
CLARE-ViT-B (ours)		<u>28.47</u>	<u>49.50</u>	<u>56.85</u>	<u>25.96</u>	<u>42.85</u>	<u>48.57</u>	<u>19.38</u>	<u>31.53</u>	<u>35.48</u>
CLARE-ViT-L (ours)		29.53	50.56	56.98	28.03	47.07	53.34	21.12	35.80	40.35

5 Experiment

5.1 Evaluation Metrics

Evaluating Referring Expression Instance Retrieval (REIR) requires measuring both retrieval and localization performance within a unified framework. To achieve this, we adopt standard metrics from related tasks and introduce a novel metric tailored for REIR.

REC Metric: Precision@0.5. Referring Expression Comprehension (REC) methods typically use Precision@0.5 to evaluate localization accuracy. A prediction is considered correct if the Intersection over Union (IoU) between the predicted and ground-truth bounding boxes exceeds 0.5:

$$\text{IoU}(B_{\text{pred}}, B_{\text{gt}}) > 0.5 \quad (7)$$

TIR Metric: Recall@k. Text-to-Image Retrieval (TIR) methods are evaluated using Recall@k, which measures the fraction of queries for which the correct image appears in the top- k retrieved results. Formally, it is defined as:

$$\text{Recall@k} = \frac{1}{N} \sum_{i=1}^N \mathbb{1}[\text{GT}(i) \in \text{Top-}k(i)] \quad (8)$$

REIR Metric: BoxRecall@k (IoU> τ). To jointly evaluate retrieval and localization in the REIR task, we adopt a unified metric called *BoxRecall@k (IoU> τ)*. A prediction is considered correct if the referred object instance is ranked among the top- k candidates and its predicted bounding box sufficiently overlaps with the ground-truth. Formally, given a batch of N referring expressions, BoxRecall@k with IoU threshold τ is defined as:

$$\text{BoxRecall@k}(\tau) = \frac{1}{N} \sum_{i=1}^N \mathbb{1} \left[\text{Inst}_i \in \text{Top-}k(i) \cap \text{IoU}(B_i^{\text{pred}}, B_i^{\text{gt}}) > \tau \right] \quad (9)$$

In which, N is the total number of queries, Inst_i denotes the ground-truth object instance for the i -th query, and $\text{Top-}k(i)$ is the top- k ranked object candidates sorted by similarity to the query expression. B_i^{pred} is the predicted bounding box of the matched candidate, and B_i^{gt} is the ground-truth bounding box of the referred instance. $\text{IoU}(\cdot)$ denotes the Intersection over Union between the predicted and ground-truth boxes, and τ is the threshold controlling the localization strictness. This metric ensures that the model

must both retrieve the correct object from a large gallery and accurately localize it. By adjusting the IoU threshold (e.g., 0.5, 0.7, 0.9), we can analyze model performance under varying localization requirements.

5.2 Implementation Details

We use the ViT-B and ViT-L variants from SigLIP [54] as our model backbone. For feature extraction, we used a Transformer encoder-decoder architecture following Deformable DETR [24, 58], consisting of 6 encoder layers and 6 decoder layers. The number of object queries M is set to 900. The MORE module uses 1 shared expert for general semantics and a routed expert bank of 4 specialists. Each query activates 2 routed experts via a top-2 gating strategy, enabling targeted relation-aware representation learning.

All experiments are trained on 8 NVIDIA A800 80GB GPUs. We use the AdamW optimizer [34] with an initial learning rate of 2×10^{-4} and adopt a learning rate schedule that combines linear warm-up with step decay. During the pretraining stage, the weight decay is set to 0.05, and the per-GPU batch size is 4. In the fine-tuning stage, the weight decay is reduced to 0.0001, and the batch size is increased to 8 per-GPU to improve contrastive learning stability.

5.3 Results on REIR

Since no prior method is designed to directly solve the REIR task, we construct competitive baselines by combining existing Text-Image Retrieval (TIR) and Referring Expression Comprehension (REC) models into a two-stage pipeline. We compare them with our proposed one-stage model, CLARE.

Why REC alone is not applicable. Although REC models are effective at within-image object localization, they are fundamentally unsuitable for REIR. Directly applying an REC model to the entire gallery requires pairing each query with every image and running $N \times N$ forward passes. For example, on the 5k-query and 5k-image split of REIRCOCO, this results in 25 million inference calls, making large-scale evaluation computationally infeasible. More importantly, REC models lack a cross-image ranking mechanism. They do not output comparable scores across images, making

Table 2: Performance Comparison of Different Methods on the REC Benchmark

Models	Backbone	RefCOCO			RefCOCO+			RefCOCog	
		val	testA	testB	val	testA	testB	val-u	test-u
Two-Stage									
MAttNet [52]	RN101	76.40	80.43	69.28	64.93	70.26	56.01	66.58	67.27
CM-Att-Erase [33]	RN101	78.35	83.14	71.32	68.09	73.65	58.03	67.99	68.67
DGA [49]	VGG16	-	78.42	65.53	-	69.07	51.99	-	63.28
RvG-Tree [16]	RN101	75.06	78.61	69.85	63.51	67.45	56.66	66.95	66.51
NMTree [32]	RN101	76.41	81.21	70.09	66.46	72.02	57.52	65.87	66.44
One-stage									
CRIS [46]	RN101	70.47	73.18	66.10	62.27	68.06	53.68	59.87	60.36
LAVT [50]	Swin-B	74.46	76.89	70.94	65.81	70.97	59.23	63.34	63.62
TransVG++ [11]	ViT-B	86.28	88.37	80.97	75.39	80.45	66.28	76.18	76.30
MDETR [19]	ViT-B	86.75	89.58	81.41	79.52	84.09	70.62	81.64	80.89
Dyn.MDETR [40]	ViT-B	85.97	88.82	80.12	74.83	81.70	63.44	72.21	74.14
SimVG [9]	ViT-B	87.07	89.04	83.57	78.84	83.64	70.67	79.82	79.93
MLLM									
shikra-7B [5]	-	87.01	90.60	80.20	81.60	<u>87.40</u>	72.10	82.30	82.20
Ferret-7B [51]	-	87.49	<u>91.35</u>	82.45	<u>80.78</u>	87.38	<u>73.14</u>	<u>83.93</u>	84.76
InternVL2-8B [8]	-	87.10	91.10	80.70	<u>79.80</u>	87.90	71.40	<u>82.70</u>	82.70
CLARE (ours)	ViT-B	<u>90.22</u>	91.18	<u>88.74</u>	78.53	81.60	72.49	83.30	<u>84.91</u>
CLARE (ours)	ViT-L	91.40	91.95	89.98	80.11	83.25	74.43	86.30	86.70

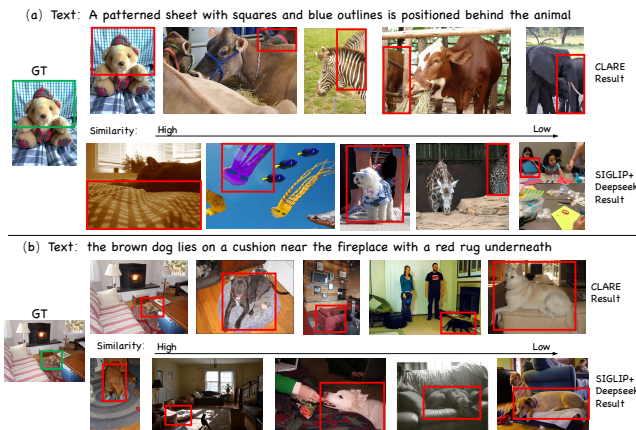


Figure 4: Qualitative comparison between CLARE and a two-stage baseline (SigLIP + DeepSeek-VL2) on REIRCOCO

it impossible to sort the gallery or determine which image most likely contains the referred instance. Therefore, REC cannot serve as a standalone baseline for REIR. **Two-stage TIR + REC strategy.** To address the above limitations, we construct a two-stage pipeline that first uses a TIR model to retrieve the most relevant images for each query, and then applies an REC model to localize the referred object within the retrieved candidates. This setup greatly reduces the number of forward passes to $2 \times N$ and is more computationally viable. **Baselines.** We evaluate three strong TIR models: CLIP [38], EVA-CLIP [41], and SigLIP [54]. For REC, we use DeepSeek-VL2 [47], a general-purpose vision-language model, and SimVG [9], a state-of-the-art REC expert. We evaluate combinations of these TIR and REC models as two-stage baselines.

Comparison with CLARE. As shown in Table 1, our proposed CLARE outperforms all combinations of two-stage baselines across

all IoU thresholds and ranking levels. Unlike the cascaded nature of two-stage methods, where failure in retrieval or localization can lead to total failure, CLARE unifies instance retrieval and localization in a single model. This end-to-end design enables more accurate cross-modal alignment and avoids cumulative errors, resulting in both better performance and lower inference cost.

Qualitative Analysis. Figure 4 shows qualitative comparisons between our proposed CLARE model and a strong two-stage baseline composed of SigLIP and DeepSeek-VL2. The examples are sampled from the REIRCOCO test set and highlight challenging referring expressions that involve spatial relations, interactions, or multi-object reasoning (e.g., *the brown dog lying on a cushion near the fireplace*). The baseline often retrieves globally similar but incorrect images due to its lack of instance-level alignment. In contrast, CLARE accurately retrieves and localizes the target object by leveraging cross-image contrastive learning and relation-aware text encoding. These results qualitatively validate the effectiveness of our end-to-end instance-level alignment strategy and highlight the advantages of modeling fine-grained semantics and inter-object relationships directly during retrieval.

5.4 Results on REC

We evaluate CLARE on three standard REC benchmarks: RefCOCO, RefCOCO+, and RefCOCog. Results are shown in Table 2. Surprisingly, although CLARE adopts a two-stream design, it performs on par with or better than many strong one-stream and MLLM-based models. We attribute this to our cross-image instance-level contrastive alignment, which allows object features to be compared across the entire batch. This encourages each instance to align closely with the referring expression not only semantically, but also in terms of position, size, and contextual relationships.

CLARE achieves particularly strong performance on RefCOCO and RefCOCog, where relational and spatial expressions are common and well-aligned with our model’s strengths. On RefCOCO+,

Table 3: TIR Performance Comparison on the REIRCOCO

Model	R@1	R@5	R@10
OpenAI CLIP	15.28	31.70	40.72
OpenAI CLIP (ViT-L)	16.79	33.80	42.43
EVA CLIP	18.57	36.12	45.19
EVA CLIP (ViT-L)	20.47	38.83	47.77
SigLIP	21.73	40.74	49.97
SigLIP (ViT-L-384)	23.25	43.10	52.01
CLARE (ViT-B)	<u>35.68</u>	<u>64.36</u>	<u>74.49</u>
CLARE (ViT-L)	36.40	65.76	75.99

Table 4: Ablation study of Two-Stage Training. Results are BR@k under IoU threshold $\tau = 0.5$.

Pretrain	Finetune	BR@1	BR@5	BR@10
✓		4.02	12.17	18.01
	✓	13.44	30.95	39.83
✓	✓	26.39	46.44	53.28

Table 5: Ablation study on MORE. Results are BR@k under IoU threshold $\tau = 0.5$.

Total	Selected	BR@1	BR@5	BR@10
0	0	26.39	46.44	53.28
2	1	26.95 (+0.56)	46.98 (+0.54)	53.96 (+0.68)
4	1	27.65 (+1.26)	47.88 (+1.44)	53.80 (+0.52)
4	2	28.47 (+2.08)	49.50 (+3.06)	56.85 (+3.57)

where such cues are intentionally minimized, our performance is slightly lower. We believe this is because the limited relational information weakens the advantage of our MORE module and contrastive learning design. Nonetheless, CLARE remains competitive even under these conditions, demonstrating its robustness and generalization ability. These results confirm that our method effectively supports both REIR and REC tasks.

5.5 Results on TIR

To assess the generalization ability of CLARE beyond REIR, we evaluate it on a standard text-to-image retrieval (TIR) setting adapted to our benchmark. Specifically, we consider a retrieval correct if the retrieved image contains the referred object instance, aligning better with the instance-level nature of our expressions.

As shown in Table 3, CLARE achieves substantial improvements over strong TIR baselines such as CLIP, EVA-CLIP, and SigLIP. For example, CLARE-ViT-L achieves 36.40% R@1, significantly surpassing the best-performing baseline SigLIP (23.25%). At R@10, CLARE reaches 75.99%, over 20 points higher than the baselines. These results suggest that CLARE is trained with instance-level supervision and explicitly aligns textual descriptions with object features, making it better suited for real-world applications where users often describe a specific object.

Table 6: Ablation study on CILA. Results are BR@k under IoU threshold $\tau = 0.5$.

Setting	BR@1	BR@5	BR@10
without CILA	4.74	14.07	21.24
mini batch CILA	18.66	39.13	48.62
CILA (Full Method)	26.39	46.44	53.28

Table 7: Ablation study on CILA loss functions. Results are BR@k under IoU threshold $\tau = 0.5$.

Loss Function	BR@1	BR@5	BR@10
Focal Loss	26.09	45.35	52.04
SigLIP Loss	26.39	46.44	53.28

5.6 Ablation Study

We conduct ablation studies using CLARE-ViT-B on the REIRCOCO test set and report BoxRecall@k under an IoU threshold of 0.5. The results verify the effectiveness of our key design components.

Effect of Training Strategy. To assess the effect of our two-phase training pipeline, we compare four settings: (1) only pre-trained, (2) directly finetuned on REIRCOCO without pretraining, and (3) our staged setup, first pre-trained on object grounding datasets, then finetuned on REIRCOCO. As shown in table 4, both pretraining and REIRCOCO fine-tuning are essential. Pretraining provides grounding capabilities, while REIRCOCO tuning enables instance-level cross-image alignment. The full staged training achieves the best results, confirming the benefit of progressive supervision.

Effect of the MORE Module. We analyze the impact of different expert routing configurations in MORE. The number of shared experts is fixed to 1, while the number of routed experts and active selection varies. The table 5 shows that enabling routed experts leads to steady performance gains. Specifically, using 4 routed experts and selecting the top-2 per query gives the best result (56.85 BR@10), confirming that relation-aware routing enhances expression-level adaptation. In contrast, disabling routed experts (i.e., 0 selected) results in 53.28 BR@10. This demonstrates that modeling diverse relational cues, such as spatial positioning, co-occurrence patterns, or relative size, is essential for resolving fine-grained expression ambiguities. See the Appendix for more details.

Effect of the CILA size. We further examine the design of the CLIA module in table 6. As the results show, removing CLIA significantly degrades performance (BR@10 drops to 21.24), indicating the necessity of contrastive supervision. Applying CLIA within minibatches improves retrieval (BR@10 = 48.62), but still falls short of the full version. Our full CLIA setting achieves the best results (BR@10 = 53.28), confirming that cross-image and cross-batch instance alignment is crucial for learning robust and discriminative visual-textual representations. It enables each object instance to be contrasted against a diverse set of negatives, leading to better generalization in large-scale retrieval scenarios.

Effect of Loss Functions in CLIA. We further examine different loss functions used within the CLIA module to guide instance-level alignment. As shown in Table 7, we compare two alternatives: Focal Loss and SigLIP Loss. Note that this setting only affects the CLIA objective, while the intra-image classification branch remains supervised with standard Focal Loss. We observe that using the SigLIP loss outperforms Focal Loss across all recall levels. These results validate our design choice in extending the SigLIP loss alignment, which is crucial for robust REIR performance.

6 Conclusion

We analyze the limitations of traditional TIR and REC tasks in handling instance-level expressions under real-world retrieval scenarios. To address this, we define a new benchmark, Referring Expression Instance Retrieval (REIR), which requires jointly retrieving and localizing object instances from an image gallery. To support research on REIR, we construct a large-scale dataset, REIRCOCO, and propose a baseline model, CLARE, which aligns visual and textual modalities via cross-image instance-level contrastive learning. CLARE achieves state-of-the-art results on REIR and shows strong generalization to existing TIR and REC tasks. REIR expands the scope of vision-language research toward fine-grained, instance-level visual understanding.

References

- [1] OpenAI: Josh Achiam, Steven Adler, Sandhini Agarwal, Lama Ahmad, Ilge Akkaya, Florencia Leoni Aleman, Diogo Almeida, Janko Altenschmidt, Sam Altman, Shyamal Anadkat, Red Avila, Igor Babuschkin, Suchir Balaji, Valerie Balcom, Paul Baletscu, Haiming Bao, Mo Bavarian, Jeff Belgum, Irwan Bello, Jake Berdine, Gabriel Bernadett-Shapiro, Christopher Berner, Lenny Bogdonoff, Oleg Boiko, Madelaine Boyd, Anna-Luisa Brakman, Greg Brockman, Tim Brooks, Miles Brundage, Kevin Button, Trevor Cai, Rosie Campbell, Andrew Cann, Brittany Carey, Chelsea Carlson, Rory Carmichael, Brooke Chan, Che Chang, Fotis Chantzis, Derek Chen, Sully Chen, Ruby Chen, Jason Chen, Mark Chen, Ben Chess, Chester Cho, Casey Chu, Hyungwon Chung, Dave Cummings, and Jeremiah Currier. 2023. GPT-4 Technical Report. (Dec 2023).
- [2] Jinze Bai, Shuai Bai, Shusheng Yang, Shijie Wang, Sinan Tan, Peng Wang, Junyang Lin, Chang Zhou, and Jingren Zhou. 2023. Qwen-VL: A Versatile Vision-Language Model for Understanding, Localization, Text Reading, and Beyond. *arXiv preprint arXiv:2308.12966* (2023).
- [3] Amulya Arun Ballakur and Arti Arya. 2020. Empirical Evaluation of Gated Recurrent Neural Network Architectures in Aviation Delay Prediction. In *2020 5th International Conference on Computing, Communication and Security (ICCCS)*, 1–7. doi:10.1109/icccs49678.2020.9276855
- [4] Nicolas Carion, Francisco Massa, Gabriel Synnaeve, Nicolas Usunier, Alexander Kirillov, and Sergey Zagoruyko. 2020. End-to-end object detection with transformers. In *ECCV*.
- [5] Keqin Chen, Zhao Zhang, Weili Zeng, Richong Zhang, Feng Zhu, and Rui Zhao. 2023. Shikra: Unleashing multimodal llm's referential dialogue magic. *arXiv preprint arXiv:2306.15195* (2023).
- [6] Xinlei Chen, Hao Fang, Tsung-Yi Lin, Ramakrishna Vedantam, Saurabh Gupta, Piotr Dollár, and C Lawrence Zitnick. 2015. Microsoft coco captions: Data collection and evaluation server. *arXiv preprint arXiv:1504.00325* (2015).
- [7] Yen-Chun Chen, Linjie Li, Licheng Yu, Ahmed El Kholy, Faisal Ahmed, Zhe Gan, Yu Cheng, and Jingjing Liu. 2020. UNITER: UNiversal Image-Text Representation Learning. 104–120. doi:10.1007/978-3-030-58577-8_7
- [8] Zhe Chen, Jiannan Wu, Wenhai Wang, Weijie Su, Guo Chen, Sen Xing, Muyan Zhong, Qinglong Zhang, Xizhou Zhu, Lewei Lu, et al. 2024. Internvl: Scaling up vision foundation models and aligning for generic visual-linguistic tasks. In *Proceedings of the IEEE/CVF Conference on Computer Vision and Pattern Recognition*. 24185–24198.
- [9] Ming Dai, Lingfeng Yang, Yihao Xu, Zhenhua Feng, and Wankou Yang. 2024. Simvg: A simple framework for visual grounding with decoupled multi-modal fusion. *Advances in neural information processing systems* 37 (2024), 121670–121698.
- [10] DeepSeek-AI DeepSeek-AI, Daya Guo, Dejian Yang, Haowei Zhang, Junxiao Song, Ruoyu Zhang, Runxin Xu, Qihao Zhu, Shirong Ma, Peiyi Wang, Xiao Bi, Xiaokang Zhang, Xingkai Yu, Yu Wu, Z.F. Wu, Zhibin Gou, Zhihong Shao, Zhuoshu Li, Ziyi Gao, Aixin Liu, Bing Xue, Bingxuan Wang, Bochao Wu, Bei Feng, Chengda Lu, Chenggang Zhao, Chengqi Deng, Chenyu Zhang, Chong Ruan, Damai Dai, Deli Chen, Dongjie Ji, Erhang Li, Fangyun Lin, Fangcong Dai, Fuli Luo, Guangbo Hao, Guanting Chen, Guowei Li, H. Zhang, Han Bao, Hanwei Xu, Haocheng Wang, Honghui Ding, Huajian Xin, Huazuo Gao, Hui Qu, Hui Li, Jianzhong Guo, Jiashi Li, Jiawei Wang, Jingchang Chen, Jingyang Yuan, Junjie Qiu, Junlong Li, J.L. Cai, Jiaqi Ni, Jian Liang, Jin Chen, Kai Dong, Kai Hu, Kaige Gao, Kang Guan, Kexin Huang, Kuai Yu, Lean Wang, Lecong Zhang, Liang Zhao, Litong Wang, Liyue Zhang, Lei Xu, Leyi Xia, Mingchuan Zhang, Minghua Zhang, Minghui Tang, Meng Li, Miaojun Wang, Mingming Li, Ning Tian, Panpan Huang, Peng Zhang, Qiancheng Wang, Qinyu Chen, Qiusi Du, Ruiqi Ge, Ruisong Zhang, Ruizhe Pan, Runji Wang, R.J. Chen, R.L. Jin, Ruyi Chen, Shanghao Lu, Shangan Zhou, Shanhuang Chen, Shengfeng Ye, Shiyu Wang, Shuiping Yu, Shunfeng Zhou, Shutong Pan, S.S. Li, Shuang Zhou, Shaoqing Wu, Shengfeng Ye, Tao Yun, Tian Pei, Tianyu Sun, T. Wang, Wangding Zeng, Wanjin Zhao, Wen Liu, Wenfeng Liang, Wenjun Gao, Wenqin Yu, Wentao Zhang, W.L. Xiao, Wei An, Xiaodong Liu, Xiaohan Wang, Xiaoakang Chen, Xiaotao Nie, Xin Cheng, Xin Liu, Xin Xie, Xingchao Liu, Xinyu Yang, Xinyuan Li, Xuecheng Su, Xuheng Lin, X.Q. Li, Xiangyue Jin, Xiaojin Shen, Xiaosha Chen, Xiaowen Sun, Xiaoxiang Wang, Xinnan Song, Xinyi Zhou, Xianzu Wang, Xinxia Shan, Y.K. Li, Y.Q. Wang, Y.X. Wei, Yang Zhang, Yanhong Xu, Yao Li, Yao Zhao, Yaofeng Sun, Yaohui Wang, Yi Yu, Yichao Zhang, Yifan Shi, Yiliang Xiong, Ying He, Yishi Piao, Yisong Wang, Yixuan Tan, Yiyang Ma, Yiyuan Liu, Yongqiang Guo, Yuan Ou, Yuduan Wang, Yue Gong, Yuheng Zou, Yujia He, Yunfan Xiong, Yuxiang Luo, Yuxiang You, Yuxuan Liu, Yuyang Zhou, Y.X. Zhu, Yanhong Xu, Yanping Huang, Yaohui Li, Yi Zheng, Yuchen Zhu, Yunxian Ma, Ying Tang, Yukun Zhu, Yuting Yan, Z.Z. Ren, Zehui Ren, Zhangli Sha, Zhe Fu, Zhean Xu, Zhenda Xie, Zhengyuan Zhang, Zhewen Hao, Zhicheng Ma, Zhigang Yan, Zhiyu Wu, Zihui Gu, Zijia Zhu, Zijun Liu, Zilin Li, Ziwei Xie, Ziyang Song, Zizheng Pan, Zhen Huang, Zhipeng Xu, Zhongyu Zhang, and Zhen Zhang. 2025. DeepSeek-R1: Incentivizing Reasoning Capability in LLMs via Reinforcement Learning. (Jan 2025).
- [11] Jiajun Deng, Zhengyuan Yang, Tianlang Chen, Wengang Zhou, and Houqiang Li. 2021. Transvg: End-to-end visual grounding with transformers. In *Proceedings of the IEEE/CVF International Conference on Computer Vision (ICCV)*. 1769–1779.
- [12] Fartash Faghri, David J. Fleet, Jamie Kiros, and Sanja Fidler. 2017. VSE++: Improving Visual-Semantic Embeddings with Hard Negatives. *arXiv: Learning, arXiv: Learning* (Jul 2017).
- [13] Andrea Frome, Greg S. Corrado, Jon Shlens, Samy Bengio, Jeff Dean, Marc'Aurelio Ranzato, and Tomas Mikolov. 2013. DeViSE: A Deep Visual-Semantic Embedding Model. *Neural Information Processing Systems, Neural Information Processing Systems* (Dec 2013).
- [14] Zhe Gan, Yen-Chun Chen, Pingqing Fu, Chen Zhu, Yu Cheng, and Jingjing Liu. 2020. Large-Scale Adversarial Training for Vision-and-Language Representation Learning. *Neural Information Processing Systems, Neural Information Processing Systems* (Jun 2020).
- [15] Richang Hong, Daqing Liu, Xiaoyu Mo, Xiangnan He, and Hanwang Zhang. 2019. Learning to compose and reason with language tree structures for visual grounding. *IEEE Transactions on Pattern Analysis and Machine Intelligence (TPAMI)* (2019).
- [16] Richang Hong, Daqing Liu, Xiaoyu Mo, Xiangnan He, and Hanwang Zhang. 2022. Learning to Compose and Reason with Language Tree Structures for Visual Grounding. *IEEE Transactions on Pattern Analysis and Machine Intelligence* (Feb 2022), 684–696. doi:10.1109/tpami.2019.2911066
- [17] Andrew Howard, Mark Sandler, Grace Chu, Liang-Chieh Chen, Bo Chen, Mingxing Tan, Weijun Wang, Yukun Zhu, Ruoming Pang, Vijay Vasudevan, et al. 2019. Searching for mobilenetv3. In *ICCV*.
- [18] Zhicheng Huang, Zhaoyang Zeng, Yupan Huang, Bei Liu, Dongmei Fu, and Jianlong Fu. 2021. Seeing Out of the bOX: End-to-End Pre-training for Vision-Language Representation Learning. In *2021 IEEE/CVF Conference on Computer Vision and Pattern Recognition (CVPR)*. doi:10.1109/cvpr46437.2021.01278
- [19] Aishwarya Kamath, Mannat Singh, Yann LeCun, Gabriel Synnaeve, Ishan Misra, and Nicolas Carion. 2021. MDETR-modulated detection for end-to-end multimodal understanding. In *Proceedings of the IEEE/CVF International Conference on Computer Vision (ICCV)*. 1780–1790.
- [20] Sahar Kazemzadeh, Vicente Ordonez, Mark Matten, and Tamara Berg. 2014. Referitgame: Referring to objects in photographs of natural scenes. In *Proceedings of the 2014 conference on empirical methods in natural language processing (EMNLP)*. 787–798.
- [21] Won-Jae Kim, Bokyung Son, and Ildoo Kim. 2021. ViLT: Vision-and-Language Transformer Without Convolution or Region Supervision. *International Conference on Machine Learning, International Conference on Machine Learning* (Feb 2021).
- [22] Thomas Kipf and Max Welling. 2016. Semi-Supervised Classification with Graph Convolutional Networks. *arXiv: Learning, arXiv: Learning* (Sep 2016).
- [23] Kuang-Huei Lee, Xi Chen, Gang Hua, Houdong Hu, and Xiaodong He. 2018. Stacked Cross Attention for Image-Text Matching. 212–228. doi:10.1007/978-3-030-01225-0_13

- [24] Feng Li, Hao Zhang, Shilong Liu, Jian Guo, Lionel M Ni, and Lei Zhang. 2022. DN-DETR: Accelerate detr training by introducing query denoising. In *CVPR*.
- [25] Junnan Li, Dongxu Li, Caimeing Xiong, and Steven Hoi. 2022. Blip: Bootstrapping language-image pre-training for unified vision-language understanding and generation. In *International conference on machine learning*. PMLR, 12888–12900.
- [26] Kungpeng Li, Yulun Zhang, Kai Li, Yuanyuan Li, and Yun Fu. 2019. Visual Semantic Reasoning for Image-Text Matching. In *2019 IEEE/CVF International Conference on Computer Vision (ICCV)*. doi:10.1109/iccv.2019.00475
- [27] Liunian Harold Li, Pengchuan Zhang, Haotian Zhang, Jianwei Yang, Chunyuan Li, Yiyu Zhong, Lijuan Wang, Lu Yuan, Lei Zhang, Jenq-Neng Hwang, et al. 2022. Grounded language-image pre-training. In *CVPR*.
- [28] Tsung-Yi Lin, Priya Goyal, Ross Girshick, Kaiming He, and Piotr Dollár. 2017. Focal loss for dense object detection. In *ICCV*.
- [29] Tsung-Yi Lin, Michael Maire, Serge Belongie, James Hays, Pietro Perona, Deva Ramanan, Piotr Dollár, and C. Lawrence Zitnick. 2014. *Microsoft COCO: Common Objects in Context*. 740–755. doi:10.1007/978-3-319-10602-1_48
- [30] Tsung-Yi Lin, Michael Maire, Serge J. Belongie, Lubomir D. Bourdev, Ross B. Girshick, James Hays, Pietro Perona, Deva Ramanan, Piotr Dollár, and C. Lawrence Zitnick. 2014. Microsoft COCO: Common Objects in Context. In *ECCV*.
- [31] Chunxiao Liu, Zhendong Mao, An-An Liu, Tianzhu Zhang, Bin Wang, and Yongdong Zhang. 2019. Focus Your Attention: A Bidirectional Focal Attention Network for Image-Text Matching. *Cornell University - arXiv, Cornell University - arXiv* (Sep 2019).
- [32] Daqing Liu, Hanwang Zhang, Feng Wu, and Zheng-Jun Zha. 2019. Learning to assemble neural module tree networks for visual grounding. In *Proceedings of the IEEE/CVF International Conference on Computer Vision (ICCV)*. 4673–4682.
- [33] Xihui Liu, Zihao Wang, Jing Shao, Xiaogang Wang, and Hongsheng Li. 2019. Improving referring expression grounding with cross-modal attention-guided erasing. In *Proceedings of the IEEE/CVF Conference on Computer Vision and Pattern Recognition (CVPR)*. 1950–1959.
- [34] Ilya Loshchilov and Frank Hutter. 2017. Decoupled Weight Decay Regularization. *Learning, Learning* (Nov 2017).
- [35] Varun K Nagராaja, Vlad I Morariu, and Larry S Davis. 2016. Modeling context between objects for referring expression understanding. In *Proceedings of the European Conference on Computer Vision (ECCV)*. Springer, 792–807.
- [36] Hyeonseob Nam, Jung-Woo Ha, and Jeonghee Kim. 2017. Dual Attention Networks for Multimodal Reasoning and Matching. In *2017 IEEE Conference on Computer Vision and Pattern Recognition (CVPR)*. doi:10.1109/cvpr.2017.232
- [37] Alec Radford, JongWook Kim, Chris Hallacy, A. Ramesh, Gabriel Goh, Sandhini Agarwal, Girish Sastry, Askell Amanda, Pamela Mishkin, Jack Clark, Gretchen Krueger, and Ilya Sutskever. 2021. Learning Transferable Visual Models From Natural Language Supervision. *Cornell University - arXiv, Cornell University - arXiv* (Feb 2021).
- [38] Alec Radford, Jong Wook Kim, Chris Hallacy, Aditya Ramesh, Gabriel Goh, Sandhini Agarwal, Girish Sastry, Amanda Askell, Pamela Mishkin, Jack Clark, et al. 2021. Learning transferable visual models from natural language supervision. In *International conference on machine learning*. PmlR, 8748–8763.
- [39] Shaoqing Ren, Kaiming He, Ross Girshick, and Jian Sun. 2015. Faster R-CNN: Towards Real-Time Object Detection with Region Proposal Networks. In *Advances in Neural Information Processing Systems (NIPS)*.
- [40] Fengyuan Shi, Ruopeng Gao, Weilin Huang, and Limin Wang. 2022. Dynamic MDETR: A Dynamic Multimodal Transformer Decoder for Visual Grounding. (Sep 2022).
- [41] Quan Sun, Yuxin Fang, Ledell Wu, Xinlong Wang, and Yue Cao. 2023. EVA-CLIP: Improved Training Techniques for CLIP at Scale. *arXiv preprint arXiv:2303.15389* (2023).
- [42] Ashish Vaswani, Noam Shazeer, Niki Parmar, Jakob Uszkoreit, Llion Jones, Aidan N Gomez, Łukasz Kaiser, and Illia Polosukhin. 2017. Attention is all you need. *Advances in Neural Information Processing Systems (NeurIPS)* 30 (2017).
- [43] Wenhui Wang, Hangbo Bao, Li Dong, Johan Björck, Zhiliang Peng, Qiang Liu, Kriti Aggarwal, Owais Khan Mohammed, Saksham Singhal, Subhojit Som, et al. 2022. Image as a Foreign Language: BEiT Pretraining for All Vision and Vision-Language Tasks. *arXiv preprint arXiv:2208.10442* (2022).
- [44] Yaxiong Wang, Hao Yang, Xueming Qian, Lin Ma, Jing Lu, Biao Li, and Xin Fan. 2019. Position Focused Attention Network for Image-Text Matching. *Cornell University - arXiv, Cornell University - arXiv* (Jul 2019).
- [45] Zihao Wang, Xihui Liu, Hongsheng Li, Lu Sheng, Junjie Yan, Xiaogang Wang, and Jing Shao. 2019. CAMP: Cross-Modal Adaptive Message Passing for Text-Image Retrieval. In *2019 IEEE/CVF International Conference on Computer Vision (ICCV)*. doi:10.1109/iccv.2019.00586
- [46] Zhaoqing Wang, Yu Lu, Qiang Li, Xunqiang Tao, Yandong Guo, Mingming Gong, and Tongliang Liu. 2022. Cris: Clip-driven referring image segmentation. In *Proceedings of the IEEE/CVF conference on computer vision and pattern recognition*. 11686–11695.
- [47] Zhiyu Wu, Xiaokang Chen, Zizheng Pan, Xingchao Liu, Wen Liu, Damai Dai, Huazuo Gao, Yiyang Ma, Chengyue Wu, Bingxuan Wang, Zhenda Xie, Yu Wu, Kai Hu, Jiawei Wang, Yaofeng Sun, Yukun Li, Yishi Piao, Kang Guan, Aixin Liu, Xin Xie, Yuxiang You, Kai Dong, Xingkai Yu, Haowei Zhang, Liang Zhao, Yisong Wang, and Chong Ruan. 2024. DeepSeek-VL2: Mixture-of-Experts Vision-Language Models for Advanced Multimodal Understanding. arXiv:2412.10302 [cs.CV] <https://arxiv.org/abs/2412.10302>
- [48] Sibe Yang, Guanbin Li, and Yizhou Yu. 2019. Dynamic graph attention for referring expression comprehension. In *Proceedings of the IEEE/CVF international conference on computer vision*. 4644–4653.
- [49] Sibe Yang, Guanbin Li, and Yizhou Yu. 2019. Dynamic graph attention for referring expression comprehension. In *Proceedings of the IEEE/CVF International Conference on Computer Vision (ICCV)*. 4644–4653.
- [50] Zhao Yang, Jiaqi Wang, Yansong Tang, Kai Chen, Hengshuang Zhao, and Philip HS Torr. 2022. Lavt: Language-aware vision transformer for referring image segmentation. In *Proceedings of the IEEE/CVF conference on computer vision and pattern recognition*. 18155–18165.
- [51] Haoxuan You, Haotian Zhang, Zhe Gan, Xianzhi Du, Bowen Zhang, Zirui Wang, Liangliang Cao, Shih-Fu Chang, and Yinfei Yang. 2023. Ferret: Refer and ground anything anywhere at any granularity. *arXiv preprint arXiv:2310.07704* (2023).
- [52] Licheng Yu, Zhe Lin, Xiaohui Shen, Jimei Yang, Xin Lu, Mohit Bansal, and Tamara L Berg. 2018. MATTNet: Modular attention network for referring expression comprehension. In *Proceedings of the IEEE conference on computer vision and pattern recognition*. 1307–1315.
- [53] Licheng Yu, Patrick Poirson, Shan Yang, Alexander C Berg, and Tamara L Berg. 2016. Modeling context in referring expressions. In *Computer Vision—ECCV 2016: 14th European Conference, Amsterdam, The Netherlands, October 11–14, 2016, Proceedings, Part II 14*. Springer, 69–85.
- [54] Xiaohua Zhai, Basil Mustafa, Alexander Kolesnikov, and Lucas Beyer. 2023. Sig-moid loss for language image pre-training. In *Proceedings of the IEEE/CVF international conference on computer vision*. 11975–11986.
- [55] Kun Zhang, Zhendong Mao, Quan Wang, and Yongdong Zhang. [n. d.]. Negative-Aware Attention Framework for Image-Text Matching. ([n. d.]).
- [56] Xingyi Zhou, Rohit Girdhar, Armand Joulin, Philipp Krähenbühl, and Ishan Misra. 2022. Detecting twenty-thousand classes using image-level supervision. In *ECCV*.
- [57] Chaoyang Zhu, Yiyi Zhou, Yunhang Shen, Gen Luo, Xingjia Pan, Mingbao Lin, Chao Chen, Liujuan Cao, Xiaoshuai Sun, and Rongrong Ji. 2022. SeqTr: A simple yet universal network for visual grounding. In *European Conference on Computer Vision (ECCV)*. Springer, 598–615.
- [58] Xizhou Zhu, Weijie Su, Lewei Lu, Bin Li, Xiaogang Wang, and Jifeng Dai. 2020. Deformable detr: Deformable transformers for end-to-end object detection. *arXiv preprint arXiv:2010.04159* (2020).

A Training

A.1 Training Process

The detailed training settings for CLARE are summarized in Table 8. Our training procedure consists of two main stages: (1) grounding pretraining and (2) REIR-specific finetuning. In each stage, we adopt the StepLR scheduler, where the learning rate decays by a factor of 10 at scheduled steps.

Stage 1: Grounding Pretraining. To equip the model with basic object grounding capabilities, we first pretrain CLARE on a combination of object detection and referring expression comprehension datasets. Specifically, we use MSCOCO [30] for detection supervision, and RefCOCO [20], RefCOCO+ [20], and RefCOCOg [35] for REC supervision. We train for 12 epochs in total, with the learning rate dropped after 10 epochs. Multi-scale training is enabled during this stage: images are resized so that the shortest side is between 480 and 800 pixels, while the longest side does not exceed 1333 pixels. AdamW is used as the optimizer with a base learning rate of 5×10^{-5} and weight decay of 0.05.

Stage 2: REIR Finetuning. We then finetune CLARE on the REIRCOCO dataset for 20 epochs. Each training batch samples 8 images with 16 object instances and their corresponding referring expressions. We retain the same multi-scale strategy as in pretraining, and continue using the StepLR scheduler. The model is trained with both retrieval loss ($\mathcal{L}_{\text{retrieve}}$) and localization loss (\mathcal{L}_{box}), with loss weights empirically set to 1.0 and 5.0, respectively. For efficient training on large-scale data, we follow Detic [56] to adopt multi-task sampling across GPUs—each GPU processes different subsets of referring expressions per iteration.

Additional Techniques. To ensure stability and consistency across image domains, we apply standard data augmentations including random horizontal flipping, color jitter, and scale jittering. Mixed precision training is enabled to reduce the memory footprint. During training, we also construct negative pairs by sampling mismatched expression-instance combinations to enhance contrastive discrimination. The total training takes approximately 100K iterations using 8 NVIDIA A100 GPUs with a batch size of 64.

A.2 Loss Functions

For training the proposed CLARE model on the REIR task, we adopt a combination of retrieval and localization losses to jointly optimize cross-modal instance alignment and spatial localization.

$\mathcal{L}_{\text{focal}}$. To supervise the instance-text matching, we adopt a Focal Loss-based formulation for the retrieval objective. Given the raw similarity score s between a textual query and a visual instance, the matching probability p is computed as $p = \sigma(s)$, where σ denotes the sigmoid function. The retrieval loss is then formulated as:

$$\mathcal{L}_{\text{focal}}(p_t) = -\alpha_t(1 - p_t)^\gamma \log(p_t), \quad (10)$$

where

$$p_t = \begin{cases} p & \text{if the instance matches the expression,} \\ 1 - p & \text{otherwise.} \end{cases} \quad (11)$$

We set $\gamma = 2$ and $\alpha_t = 0.25$ following [28].

\mathcal{L}_{box} . For precise instance localization, we use a combination of GIoU loss and ℓ_1 loss as in DETR-based frameworks [4, 58]:

$$\mathcal{L}_{\text{box}}(b, \hat{b}) = \lambda_{\text{giou}} \mathcal{L}_{\text{giou}}(b, \hat{b}) + \lambda_{L_1} \|b - \hat{b}\|, \quad (12)$$

$$\mathcal{L}_{\text{giou}}(b, \hat{b}) = 1 - \text{IoU}(b, \hat{b}) + \frac{A^c(b, \hat{b}) - U(b, \hat{b})}{A^c(b, \hat{b})}, \quad (13)$$

where $A^c(b, \hat{b})$ is the area of the smallest enclosing box, and $U(b, \hat{b})$ is the union area of b and \hat{b} .

The final training objective is a weighted sum:

$$\mathcal{L} = \mathcal{L}_{\text{retrieve}} + \mathcal{L}_{\text{box}}. \quad (14)$$

B Datasets

B.1 Origin Datasets

RefCOCO/+/g. RefCOCO [20, 53] contains 142,210 referring expressions, 50,000 referred objects, and 19,994 images. The testA set primarily describes people, while the testB set mainly describes objects other than people.

RefCOCO+ contains 141,564 expressions, 49,856 referred objects, and 19,992 images. RefCOCO+ referring expressions focus more on attributes of the referent, such as color, shape, and digits, and avoid using words indicating absolute spatial location.

RefCOCOg [47; 48] is divided into two partitions: the google split and the umd split. Each split includes 95,010 referring expressions, 49,822 referred objects, and 25,799 images.

MS COCO Dataset The Microsoft Common Objects in Context (MS COCO) dataset [29] is a large-scale image dataset developed by Microsoft to advance research in object recognition within complex, real-world scenes. It contains over 330,000 images, with more than 200,000 of them annotated in detail. These annotations span 80 object categories and 91 “stuff” categories, comprising over 1.5 million labeled instances. Each image contains an average of 7.7 object instances, making the dataset particularly suitable for tasks that require understanding of rich contextual information. MS COCO supports multiple computer vision tasks, including object detection, instance segmentation, keypoint detection, and image captioning, and is widely used as a benchmark for evaluating model performance in real-world settings.

The MS COCO Captions dataset is a curated subset of MS COCO specifically designed for image captioning tasks. It provides five human-written captions for each image in the training and validation splits, totaling over 1.5 million captions. In addition, the dataset includes a “c40” subset, where each image is associated with 40 diverse captions, aiming to improve evaluation robustness. An official evaluation server is provided with support for standard captioning metrics such as BLEU, METEOR, ROUGE, and CIDEr, establishing MS COCO Captions as a standard benchmark for image-to-text generation.

The MS COCO Detection subset focuses on object detection, offering precise bounding box annotations and category labels for the 80 object classes. Compared to other datasets, COCO Detection images exhibit more cluttered scenes, higher object density, and a greater proportion of small objects, making the detection task significantly more challenging. Evaluation is conducted using Average Precision (AP) and Average Recall (AR) across multiple

Stage	Task	Dataset	Sampling Weight	Batch Size	Short	Long	Num GPU	Lr	Max Iter	Step
pretraining	OD&REC	COCO [30] RefCOCO [20]	1	8	480 ~ 800	1333	8	0.0002	60000	48000
finetune	REIR	REIRCOCO	1	4	480 ~ 800	1333	8	0.0002	60000	48000

Table 8: Ingredients and hyper-parameters for our training.

Intersection-over-Union (IoU) thresholds, providing a comprehensive assessment of detection accuracy.

B.2 REIRCOCO Construction

GPT4o. To construct high-quality referring expressions for the REIRCOCO dataset, we utilize GPT-4o to generate fine-grained descriptions for each object instance. The generation process is guided by a carefully designed prompt that ensures **accuracy**, **uniqueness**, and **referential clarity**. Given an image and its associated annotation data—including object instances with bounding boxes and image-level captions—the model is instructed to generate **five distinct natural language descriptions** for each object.

Each generated description:

- Relies solely on visual and semantic cues explicitly present in the image and annotations;
- Is designed to uniquely identify the target object among many similar instances across different images;
- Emphasizes actions, relationships, and spatial configurations, while avoiding direct coordinate references;
- Follows a concise, natural, human-like style with short sentences and minimal punctuation;
- Encourages diversity without referencing prior descriptions or repeating identical patterns.

For instances that are heavily occluded, blurry, or too small to be recognized due to a minimal bounding box, the description "Instance quality is poor." is returned. This generation pipeline enables REIRCOCO to support precise instance-level retrieval and grounding by providing **rich, contextualized, and discriminative** textual descriptions.

See Figure 9 for an illustration of the dataset generation process.

Deepseek R1. After generating candidate descriptions for each object instance using GPT-4o, we adopt a filtering stage based on DeepSeek-VL R1 to ensure the quality, uniqueness, and referential clarity of the descriptions. The filtering process is guided by a structured prompt, which instructs the model to verify whether each generated description is accurate, unambiguous, and grounded solely in the provided image and annotations.

Filtering Protocol.

- Each input consists of an image, a set of object instances with bounding boxes and semantic labels (in JSON format), and multiple candidate descriptions for each instance.
- The model is prompted to evaluate whether each description:
 - Is factually accurate based on the image and annotation.
 - Uniquely identifies the target object instance among many similar instances.
 - Avoids hallucinated content or unverifiable assumptions.
 - Uses the target object as the subject of the sentence.
 - Follows a natural and concise linguistic style.

- Descriptions that are vague, ambiguous, redundant, or based on content not explicitly present in the image are discarded.
- If the object is heavily occluded, blurry, or too small to be reliably described, the model returns the placeholder sentence: "Instance quality is poor."

Output Format. The final output remains in JSON format, with each valid instance entry containing an `instances_id` field and a list of verified high-quality descriptions. Each instance is guaranteed to have up to five unique, human-like descriptions that are referentially discriminative and semantically grounded.

This filtering stage significantly improves the reliability and precision of the REIRCOCO dataset by eliminating noisy or under-specified referring expressions. See Figure 10 for an illustration of the dataset generation process. Although DeepSeek cannot accept images as input, it possesses strong reasoning capabilities. Relying solely on captions and GPT-generated descriptions, it can effectively perform filtering. We showcase part of DeepSeek’s output in the figure ??.

B.3 REIRCOCO Visualization

Due to space limitations in the main text, we present here the full generation process of all instances for a single image, as shown in the figure 5

C REIR Visualization

C.1 CLARE Result

Qualitative Analysis of Failure Cases. Figure 8 presents representative failure cases of our CLARE model on the REIRCOCO test set. Most errors occur when the referring expression involves complex relations, fine-grained distinctions, or ambiguous linguistic constructs. For example, queries such as “the boy sitting behind the girl wearing a red hat” or “the leftmost chair next to the broken table” require the model to jointly understand spatial layouts, relative positions, and object interactions across cluttered scenes.

We observe that CLARE occasionally retrieves a visually similar instance but misinterprets relational cues, leading to incorrect localization. These errors often arise in scenes with multiple similar objects or when relation keywords are subtle or implicit. Additionally, in cases where the expression refers to rare object configurations not well-covered in training (e.g., overlapping small objects), the model may produce high similarity scores for incorrect regions.

These observations highlight the challenge of grounding relational and compositional semantics in open-world settings and suggest future work on enhancing reasoning over multi-object contexts and rare cases.

We also present a number of qualitative examples. Since these examples are composed from images directly during testing, some of them may appear slightly misaligned or irregular.

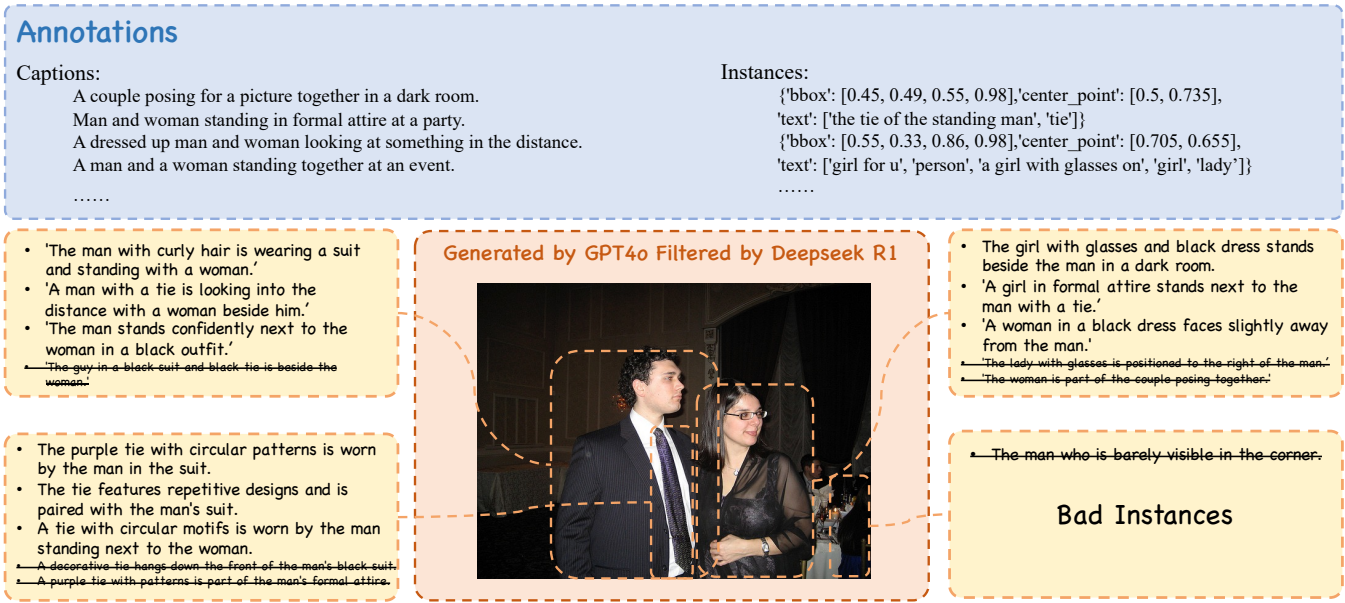


Figure 5: The data construction process for all instances in a single image

The sandwich is positioned centrally with visible vegetables and pickles



Giraffe stands prominently, chewing foliage in mid-frame



Figure 7: Some failure cases of CLARE on the REIRCOCO dataset

GT

the rightmost skater has dark shoes with white laces



GT

compact vehicle positioned left of the red mini van in the parking area



GT

the shortest back row player wears white at the central position



GT

long haired child engages with game controller in living room



GT

a black chair positioned against the wall supports the woman and her dogs



Figure 8: The qualitative results of CLARE on REIRCOCO. This result demonstrates that CLARE can effectively retrieve and localize target objects from image galleries based on textual queries.

```
Analyze the given image captioning data and generate multiple detailed descriptions for each object ('instance') found in the image. Each description must be accurate and unique, focusing solely on the information available in the image and annotations. Do not include any information that is not explicitly present in the image or annotation data. The descriptions should ensure that the object can be uniquely identified from a large set of similar images.
# Steps
1. Data Preparation:
  - Input consists of an image, and its annotation in JSON format that includes 'instances' and 'captions'.
  - 'instances' provide information about the majority of the objects in the image with bounding box and semantic details.
  - 'captions' provide multiple sentences describing the image.
2. Description Generation:
  - For each object in 'instances':
    - Generate concise, clear descriptions.
    - Focus exclusively on using:
      - The object's inherent properties.
      - Actions or relationships it has with other objects.
      - Spatial location relationships.
      - Semantic information that appears in the image and can be referenced.
    - Ensure each description allows the object to be uniquely identifiable.
    - Ensure diversity without referencing prior descriptions.
    - Avoid direct mention of coordinate values.
  - For instances that are heavily occluded, blurry, or too small to be recognized due to a tiny bounding box, directly return "Instance quality is poor."
3. Description Style:
  - Use short sentences.
  - Minimize commas, avoid long or complex sentences.
  - Each description must reflect the interesting, accurate, and clear representation of the object, emphasizing the object as the focal point.
  - Each description should be more natural and aligned with human language conventions.
  - Descriptions should lean towards referencing additional objects present in the image, ensuring that among many similar images, the uniquely matching image can be accurately identified.
  - If the target object lacks rich semantic information, it can be identified by describing a semantically rich object in the image and specifying its relationship with the target object.
  - Each description must use the described object as the subject of the sentence.
# Output Format
Output must be in JSON format containing a list of generated descriptions for each instance in the following format:
- instances_id: Identifier for the object.
- description: A list of descriptions, where each description is designed to uniquely describe the object.
# Examples
## Input
pass
## Output:
pass
(Note: Real examples will include more descriptions for each object and use exact identifiers from the input data,It should ensure that 5 descriptions are generated for each instance.)
`
# Notes
- Generate at least 5 unique descriptions for each object.
- Each description should enable easy identification and retrieval of the object from multiple images.
- Focus on the object's uses, relationships, and other deep semantic information—not just appearance.
- For instances that are heavily occluded, blurry, or too small to be recognized due to a tiny bounding box, directly return "Instance quality is poor."
```

Figure 9: Prompt used for generating textual descriptions with GPT-4o

```

# Task: Enhance Object Descriptions for Image Retrieval
You will receive a JSON object containing:
- `captions`: High-level descriptions of the overall scene context. Use them to understand the context but do not include them in your output.
- `instances`: Objects within the scene, each including:
  - A unique `instances_id`.
  - Five initial descriptions of the same object from different viewpoints.
Your goal is to optimize these descriptions to make them clearer, more detailed, and distinctive while keeping them accurate and natural. The main
subject of all descriptions for a specific object must always remain the object itself, and the descriptions must remain consistent and
straightforward. Do not miss any object, the number of objects output should be the same as the number of objects input.
## Processing Steps
### 1. Analyze Context
- Carefully read all `captions` and `instances` descriptions.
- Clearly understand each object and its context.
- Do NOT introduce new objects or relationships not mentioned or implied.
### 2. Enhance or Retain Descriptions
- Keep descriptions unchanged if they are already clear, detailed, and naturally phrased.
- Improve descriptions only if they are vague, unclear, repetitive, or unnatural.
- Combine similar or repetitive descriptions to form concise and informative ones.
### 3. Remove Unhelpful Descriptions
- Delete descriptions only if they are:
  - Unclear and can't be improved using provided information.
  - Redundant or not uniquely identifying the object.
  - If none of the descriptions for the object meet the requirements, return "None of the descriptions are suitable."
### 4. Simplicity and Naturalness
- Prefer simple vocabulary and short sentences.
- Ensure all descriptions sound natural, like human speech.
- Keep the subject consistent across descriptions for each object.
## Output Format
Return a JSON object exactly matching the input instances structure (no instances omitted or added):
**Important Notes:**
- The number of descriptions per instance may vary, but each original instance must appear exactly once.
- If an original description is already clear, natural, and detailed, keep it unchanged.
## Example
### Input
pass
### Output
pass
## Key Guidelines
- Do not add new details: Only refine given information.
- Simple language: Always prefer easy and clear words.
- Natural descriptions: Write as naturally as possible.
- Consistency: Maintain the object as the main subject consistently across descriptions.
- Distinctiveness: Ensure each description uniquely helps in identifying the object clearly.
- Do not miss any object: The number of objects output should be the same as the number of objects input.

```

Figure 10: Prompt used for filtering textual descriptions with DeepSeek R1

